High-sensitivity compact ultrasonic detector based on a pi-phase-shifted fiber Bragg grating

Amir Rosenthal,* Daniel Razansky, and Vasilis Ntziachristos

Institute for Biological and Medical Imaging (IBMI), Technical University of Munich and Helmholtz Center Munich, Ingoldstädter Landstrasse 1, 85764 Neuherberg, Germany

**Corresponding author: amir.rozental@helmholtz-muenchen.de*

Received February 9, 2011; revised March 22, 2011; accepted April 4, 2011; posted April 14, 2011 (Doc. ID 142366); published May 9, 2011

A highly sensitive compact hydrophone, based on a pi-phase-shifted fiber Bragg grating, has been developed for the measurement of wideband ultrasonic fields. The grating exhibits a sharp resonance, whose centroid wavelength is pressure sensitive. The resonance is monitored by a continuous-wave (CW) laser to measure ultrasound-induced pressure variations within the grating. In contrast to standard fiber sensors, the high finesse of the resonance—which is the reason for the sensor's high sensitivity—is not associated with a long propagation length. Light localization around the phase shift reduces the effective size of the sensor below that of the grating and is scaled inversely with the resonance spectral width. In our system, an effective sensor length of 270 μm, pressure sensitivity of 440 Pa, and effective bandwidth of 10 MHz were achieved. This performance makes our design attractive for medical imaging applications, such as optoacoustic tomography, in which compact, sensitive, and wideband acoustic detectors are required. © 2011 Optical Society of America

OCIS codes: 060.2370, 060.3735, 170.7170.

The detection of ultrasonic fields is conventionally performed using piezoelectric sensors. One of the main drawbacks of these sensors is their sensitivity, which is proportional to detection area. This readily limits applications in which small sensors are required. In addition, piezoelectric sensors may also be ferroelectric and pyroelectric, e.g., polyvinylidene fluoride. Those materials are very sensitive to electromagnetic disturbances, complicating their use in hybrid application involving electromagnetic sources, such as optoacoustic tomography [1] and thermoacoustic tomography. Here the strong electromagnetic radiation of the laser or microwave source may interfere with the acoustic detection.

An alternative to piezoelectric sensors is the detection of ultrasound by optical means. The underpinning of optical detection of ultrasound is that variations in pressure in the medium transmitting the optical fields lead to change in the phase they accumulate. The detection of this phase has been demonstrated by using several techniques, including etalons [2], Mach–Zehnder interferometers [3–5], passive fiber Bragg gratings (FBGs) [6,7], and distributed feedback (DFB) fiber grating lasers [8,9]. These optical detectors, in contrast to piezoelectric detectors, are inherently immune to electric interference, limiting cross talk in hybrid modalities. Furthermore, fiber-based detectors offer an additional advantage of small size and mechanical flexibility.

One of the determining factors of the sensitivity in optical detection is the efficiency in which pressure is converted to phase variation. This efficiency depends upon the optical properties of the guiding medium, e.g., strain optic coefficient, and on the optical path of the sensing elements. As a result, there is an inherent trade-off between the sensitivity and length of optical sensors, which is analogous to the trade-off between sensitivity and area in piezoelectric detectors. This trade-off can be mitigated by using materials with high strain optic coefficients [4], or by using fibers folded in small areas [3]. Despite improvements in the field, current fiber-optic sensors are still unfit for demanding applications, such as intravascular optoacoustic applications, owing to either their size or sensitivity.

In this Letter, we demonstrate a fiber-optic ultrasound detector based on monitoring the reflection of a narrow linewidth CW laser from an FBG with a pi-phase shift in its center. Such gratings exhibit strong resonances obtained at frequencies within the optical bandgap. The resonant effect is advantageous for ultrasound sensing for two reasons: First, light at resonance frequencies undergoes strong localization centered on the phase shift, which allows achieving very small sensing lengths. Second, the resonance frequencies exhibit a slow-light effect, i.e., the group delay is significantly higher than what would be obtained if propagated in a fiber of a same length. Accordingly, the resonance increases the effective optical path length. Thus, in pi-phase-shifted FBGs there is an inverse relationship between the optical path length, which determines sensitivity, and the effective sensing length.

The hallmark of pi-phase-shifted FBGs is the narrow transmission resonance in the middle of their otherwise totally reflecting bandgap. The reflection spectrum of pi-phase-shifted FBGs can be calculated using the transfer-matrix method [10]:

$$r_g = \frac{2k}{\kappa}\left[\left(\frac{\gamma}{\kappa \tanh \gamma L/2} - \frac{ik}{\kappa}\right)^2 - 1\right]^{-1}, \tag{1}$$

where $k = 2\pi(\lambda - 2n\Lambda)/\lambda^2$ is the wavenumber detuning, λ is wavelength, n is the refractive index of the optical fiber, Λ is the grating period, κ is the coupling coefficient, $\gamma = \sqrt{\kappa^2 - k^2}$, and L is the grating length. According to Eq. (1), the transmission resonance is centered on $k = 0$ ($\lambda = 2n\Lambda$), which corresponds to a reflection of $r_g = 0$. Variations in either n or Λ due to external perturbations can thus cause the resonance wavelength to shift. Assuming $\kappa L \gg 1$, the full width at half-maximum (FWHM) of the resonance in $|r_g|^2$ can be obtained from Eq. (1) and is given by $\Delta k = 4\kappa \exp(-\kappa L)$. Using the transfer-matrix method, the field within the grating can be

 © 2011 Optical Society of America

calculated. Assuming $\kappa L \gg 1$ and $k \le \Delta k$, the amplitude of the optical field within the grating can be approximated by

$$|u(z)| \approx \sqrt{1 - |r_g(k)|^2} e^{\kappa L/2 - \kappa |z - L/2|}, \quad (2)$$

where $z \in [0, L]$ is the coordinate along the grating length. Equation (2) shows that the maximum of the field is obtained at the center of the grating and decays exponentially from there with a rate of κ. First-order perturbation theory shows that the effect of local variations in κ on the reflection spectrum at a given wavelength are weighted by the field in the grating $u(z)$ at that wavelength [11]. When the grating is used as an ultrasound detector, the local variations in κ are proportional to the pressure induced by the acoustic field [6]. Thus, the implication of Eq. (2) is an exponential amplification of the local sensitivity of the grating to acoustic fields for the region around the phase shift. Summarizing the analytical results, the sensitivity of pi-phase-shifted FBG increases exponentially with κL, and their effective sensing length is proportional to κ^{-1}.

Figure 1 shows the experimental setup for the FBG-based acoustic sensor. The grating was immersed in water at a distance of 4.5 mm from a flat acoustic PZT transducer (Olympus) connected to a pulse generator, which produced square-wave pulses with a duration of 67 ns and voltage of 100 V–400 V in 100 V increments. The laser was a tunable CW laser with a linewidth of 8.1×10^{-4} pm (81940A, Agilent Technologies, Inc, Santa Clara, California, USA) and tuning resolution of 1 pm. The laser wavelength was tuned to the maximum slope of the grating resonance and laser power was set to 4 mW. A fused fiber coupler guided the light reflected from the grating to a fast photodiode connected to a digital oscilloscope. Thus, small variations in the wavelength of the resonance were detected by recording the reflected intensity by a photodiode.

The FBG was fabricated in a polarization-maintaining fiber with a designed length of 2.5 mm. After grating fabrication, the fiber was recoated with acrylic coating. The reflection spectrum of the unperturbed grating to unpolarizied light is shown in Fig. 2. The spectral width of the grating bandgap (>90% reflection), was equal to 1.38 nm, indicating a coupling coefficient of $\kappa = 2.58$ mm^{-1}. The figure shows two notches in the bandgap region of the spectrum, where each notch is obtained for a different polarization state. The notches reach only 50% reflectivity because for each notch, half of the laser power is in the mode orthogonal to that of the notch.

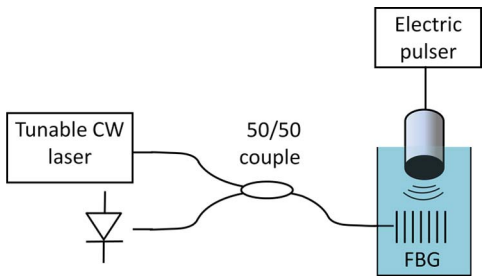

Fig. 1. (Color online) Schematic description of the detection scheme. A CW laser is used to monitor the reflection of an FBG.

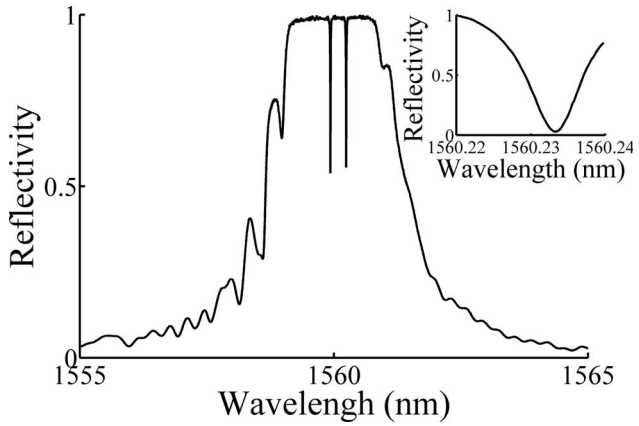

Fig. 2. Reflection spectrum of the grating, as obtained using unpolarized light. The two dips in the bandgap correspond to the two polarization modes. The inset shows in high resolution the resonance of the slow-axis polarization obtained with a polarized source. The figures are shown in linear scale.

The inset shows the spectrum of the resonance mode obtained for slow-axis polarization. The measured −3 dB bandwidth of the grating resonance was 8 pm, corresponding to $L = 2.38$ mm, in agreement with the designed value.

The acoustic field produced by the transducer was first measured using a calibrated needle hydrophone (Model HPM1/1, Precision Acoustics Ltd., Dorset, U.K.) at a distance of 4.5 mm. We found that 100 V pulse amplitude corresponded to an acoustic pressure of 175 kPa for 67 nsec pulses. Figure 3(a) shows the response of the FBG sensor to the 175 kPa acoustic pulse. The noise in the signal was assessed by analyzing the temporal regions that preceded the oscillatory pulse. The standard deviation of the noise corresponded to a pressure amplitude of 0.45 kPa for a 20 MHz bandwidth measurement. The maximum voltage signal obtained for the 100–400 V pulse amplitudes is shown as a function of acoustic pressure in the inset of Fig. 3 (round markers) and was fitted according to the shape of the resonance (dashed curve). A 20% divergence from linearity was obtained at 750 kPa.

Figure 3(b) shows the spectral response of the detector (solid curve), calculated by taking the Fourier transform of the temporal response. The spectrum exhibited

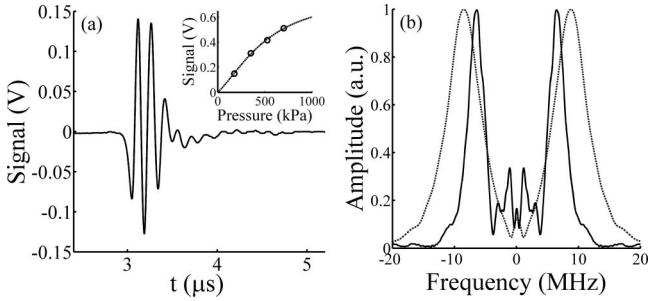

Fig. 3. (a) Temporal and (b) spectral responses (solid curves) of the optical sensor obtained for an acoustic plane wave formed by an ultrasound transducer fed with 67 ns square pulses. The inset shows the maximal voltage signal obtained as a function of acoustic pressure; at 750 kPa, 20% deviation from linear response is obtained. The spectrum of the acoustic source, as measured by the hydrophone, is shown in (b).

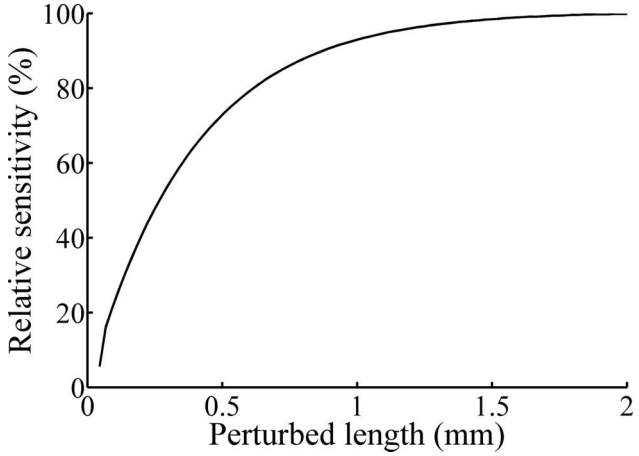

Fig. 4. Relative sensitivity of the FBG used in this work as function of the perturbed length, when the perturbation is symmetrically applied around the pi-phase jump. The figure shows that a 270 μm length is responsible for half of the grating's sensitivity.

resonant behavior with peak sensitivity at 6.5 MHz and FWHM of 3 MHz. The total bandwidth, defined as the span over which the sensitivity is above 10% of its maximum value, is equal to 10 MHz. In comparison, when the acoustic field was measured with the hydrophone (dashed curve), peak sensitivity at 8.5 MHz and FWHM bandwidth of 6 MHz were obtained.

In order to estimate the effective length of the sensing region in the FBG, we numerically simulated the spectral shift of the grating spectrum under local perturbation. The perturbation was simulated by slightly increasing the refractive index of the grating over the region of interest, though perturbation in the grating period is mathematically equivalent [7]. The perturbation was applied symmetrically around the phase shift, and the respective resonance shift was divided by the one obtained when the perturbation is applied to the entire grating length. Figure 4 shows the relative shift in the resonance as a function of the perturbed length. According to the figure, a region of 270 μm around the phase shift is responsible for 50% of the grating's sensitivity. This value corresponds to the scale of the field distribution around the phi-phase shift, which had an effective length of $\kappa^{-1} = 388\,\mu$m.

In conclusion, we demonstrated a compact fiber-optic sensor for highly sensitive wideband ultrasound measurements, suitable for optoacoustic signal detection. The sensing element was a pi-phase-shifted FBG, which exhibited a strong resonance in its bandgap frequencies. Ultrasound-induced shifts in the resonance wavelength were measured by tuning a CW laser to the resonance wavelength and monitoring the resulting reflection. One of the appealing properties of our approach is that, in contrast to the standard fiber-optic scheme, there is no trade-off between the sensitivity and length of the sensor. Conversely, owing to light localization, an inverse relation between sensitivity and effective sensor length is obtained. A similar inverse relation is expected for pi-phase-shifted FBG written in active fibers [8,9]. However, the maximum grating strength achievable in active fibers is currently lower than that achieved in passive fibers, thus imposing a longer sensing length. Additionally, DFB lasers based on pi-phase-shifted FBG exhibit relaxation oscillations [8], which may interfere with the sensor operation.

A. Rosenthal acknowledges the financial support of the European Community's Seventh Framework Programme (FP7/2007-2013) under grant agreement n° 235689. D. Razansky acknowledges support from the German Research Foundation (DFG) Research Grant (RA 1848/1) and the European Research Council Starting Grant. V. Ntziachristos acknowledges financial support from the European Research Council Advanced Investigator Award, and the Federal Ministry of Education and Research's Innovation in Medicine Award.

References

1. D. Razansky, M. Distel, C. Vinegoni, R. Ma, M. Perrimon, R. W. Koster, and V. Ntziachristos, Nat. Photon. **3**, 412 (2009).
2. P. C. Beard and T. N. Mills, Electron. Lett. **33**, 801 (1997).
3. H. Lamela, D. Gallego, and A. Oraevsky, Opt. Lett. **34**, 3695 (2009).
4. D. Gallego and H. Lamela, Opt. Lett. **34**, 1807 (2009).
5. D. R. Bacon, IEEE Trans. Ultrason. Ferroelectr. Freq. Control **35**, 152 (1988).
6. N. E. Fisher, D. J. Webb, C. N. Pannell, D. A. Jackson, L. R. Gavrilov, J. W. Hand, L. Zhang, and I. Bennion, Appl. Opt. **37**, 8120 (1998).
7. D. C. Betz, G. Thursby, B. Culshaw, and W. J. Staszewski, Smart Mater. Struct. **12**, 122 (2003).
8. C. C. Ye and R. P. Tatam, Smart Mater. Struct. **14**, 170 (2005).
9. S. W. Løvseth, J. T. Kringlebotn, E. Rønnekleiv, and K. Bløtekjær, Appl. Opt. **38**, 4821 (1999).
10. T. Erdogan, J. Lightwave Technol. **15**, 1277 (1997).
11. A. Rosenthal and M. Horowitz, J. Opt. Soc. Am. A **22**, 84 (2005).